MOLECULAR AND CELLULAR BIOLOGY, Apr. 1998, p. 1855–1865 Vol. 18, No. 4
0270-7306/98/$04.00+0

Dbp6p Is an Essential Putative ATP-Dependent RNA Helicase Required for 60S-Ribosomal-Subunit Assembly in *Saccharomyces cerevisiae*

DIETER KRESSLER,[1]* JESÚS DE LA CRUZ,[1] MANUEL ROJO,[2] AND PATRICK LINDER[1]

Département de Biochimie Médicale, Centre Médical Universitaire,[1] and Département de Biochimie, Sciences II,[2] Université de Genève, 1211 Geneva 4, Switzerland

Received 31 October 1997/Returned for modification 21 November 1997/Accepted 30 December 1997

A previously uncharacterized *Saccharomyces cerevisiae* open reading frame, YNR038W, was analyzed in the context of the European Functional Analysis Network. YNR038W encodes a putative ATP-dependent RNA helicase of the DEAD-box protein family and was therefore named *DBP6* (DEAD-box protein 6). Dbp6p is essential for cell viability. In vivo depletion of Dbp6p results in a deficit in 60S ribosomal subunits and the appearance of half-mer polysomes. Pulse-chase labeling of pre-rRNA and steady-state analysis of pre-rRNA and mature rRNA by Northern hybridization and primer extension show that Dbp6p depletion leads to decreased production of the 27S and 7S precursors, resulting in a depletion of the mature 25S and 5.8S rRNAs. Furthermore, hemagglutinin epitope-tagged Dbp6p is detected exclusively within the nucleolus. We propose that Dbp6p is required for the proper assembly of preribosomal particles during the biogenesis of 60S ribosomal subunits, probably by acting as an rRNA helicase.

In eukaryotes, ribosome biogenesis is a complex process where approximately 80 ribosomal proteins (r-proteins) and four rRNAs are assembled into mature ribosomal subunits. The 60S ribosomal subunit consists of three rRNAs (5S, 5.8S, and 25S or 28S) and approximately 45 r-proteins, whereas the 40S ribosomal subunit is formed by one 18S rRNA molecule and approximately 35 r-proteins (74). In all eukaryotes, rRNAs are synthesized as precursors (pre-rRNAs) that require maturation by a large number of nonribosomal *trans*-acting factors. Transcription of the rRNA genes, processing (cleavage and modification) of the pre-rRNAs, and assembly with r-proteins are concomitant processes that take place primarily in a specialized subnuclear compartment termed the nucleolus (35).

Although ribosome biogenesis has been extensively studied for higher eukaryotes (14), biochemical strategies and genetic approaches with the yeast *Saccharomyces cerevisiae* have provided the best-characterized picture regarding the various *cis* elements and *trans*-acting factors participating in this process (59, 60, 64, 67). In yeast, three of the four rRNAs (18S, 5.8S, and 25S) are produced as a single 35S precursor by RNA polymerase I, whereas the fourth rRNA (5S) is transcribed independently by RNA polymerase III (67, 74). In the 35S pre-rRNA, the mature rRNA sequences are separated by two internal transcribed spacers, ITS1 and ITS2, and flanked by two external transcribed spacers, 5′ ETS and 3′ ETS (Fig. 1A). During the maturation of the 35S pre-rRNA, these transcribed spacers are removed by a series of ordered endo- or exonucleolytic steps requiring small nucleolar RNAs (snoRNAs) and proteins as *trans*-acting factors (Fig. 1B) (59, 67). Concomitantly, the pre-rRNAs are also covalently modified, mostly by 2′ O methylation of ribose groups and conversion of uridine residues to pseudouridine (60). In addition to snoRNAs, enzymes for rRNA modification, and endo- and exonucleases, another class of *trans*-acting factors predicted to function enzymatically in ribosome biogenesis is the ATP-dependent RNA helicases.

RNA helicases originate from many organisms, ranging from bacteria to humans (51). They are involved in a variety of RNA metabolic processes, including translation initiation (42), pre-mRNA splicing (48), ribosome biogenesis (67), and RNA degradation (25, 34). An ATP-dependent RNA unwinding activity has been observed for some of these proteins (e.g., see references 22, 30, and 46), whereas only an RNA-dependent ATPase activity could be attributed to others (e.g., see references 17, 27, and 53). However, based on sequence analysis, most are regarded as putative ATP-dependent RNA helicases. Many putative ATP-dependent RNA helicases are grouped in the DEAD-box protein family. This family is characterized by a core region of about 300 to 350 amino acids that shows strong homology to the translation initiation factor eIF4A, which is the prototype of the DEAD-box protein family (32). The core region consists of eight motifs with strong sequence conservation among all members of the family (51). To date, biochemical properties have been attributed only to four of the motifs within the mammalian eIF4A (42). Sequence divergence within the DEAD box gives rise to the DEXH subgroup, whose members are more heterogeneous with respect to both sequence and function (16). Moreover, individual members of the family have distinct amino- and carboxy-terminal regions that vary in length (51). These regions and differences within the core region may confer substrate specificity, direct the protein to its subcellular localization, include RNA binding motifs, or bind to accessory proteins, which could by themselves carry out the aforementioned functions.

To date, nine putative RNA helicases have been shown to be implicated in ribosome biogenesis in yeast. Dbp4p, Fal1p, Rok1p, and Rrp3p are required for 18S rRNA synthesis (28, 31, 41, 65). Dbp3p, Dbp7p, Drs1p, and Spb4p are involved in 25S rRNA maturation (10, 44, 49, 72). Dob1p is required for correct 3′-end processing of the 5.8S rRNA (12). Considering their putative RNA unwinding activity, RNA helicases could play different roles during ribosomal biogenesis reactions.

* Corresponding author. Mailing address: Département de Biochimie Médicale, Centre Médical Universitaire, Université de Genève, 1 rue Michel-Servet, CH-1211 Geneva 4, Switzerland. Phone: 41 22 702 55 08. Fax: 41 22 702 55 02. E-mail: dieter.kressler@medecine.unige.ch.

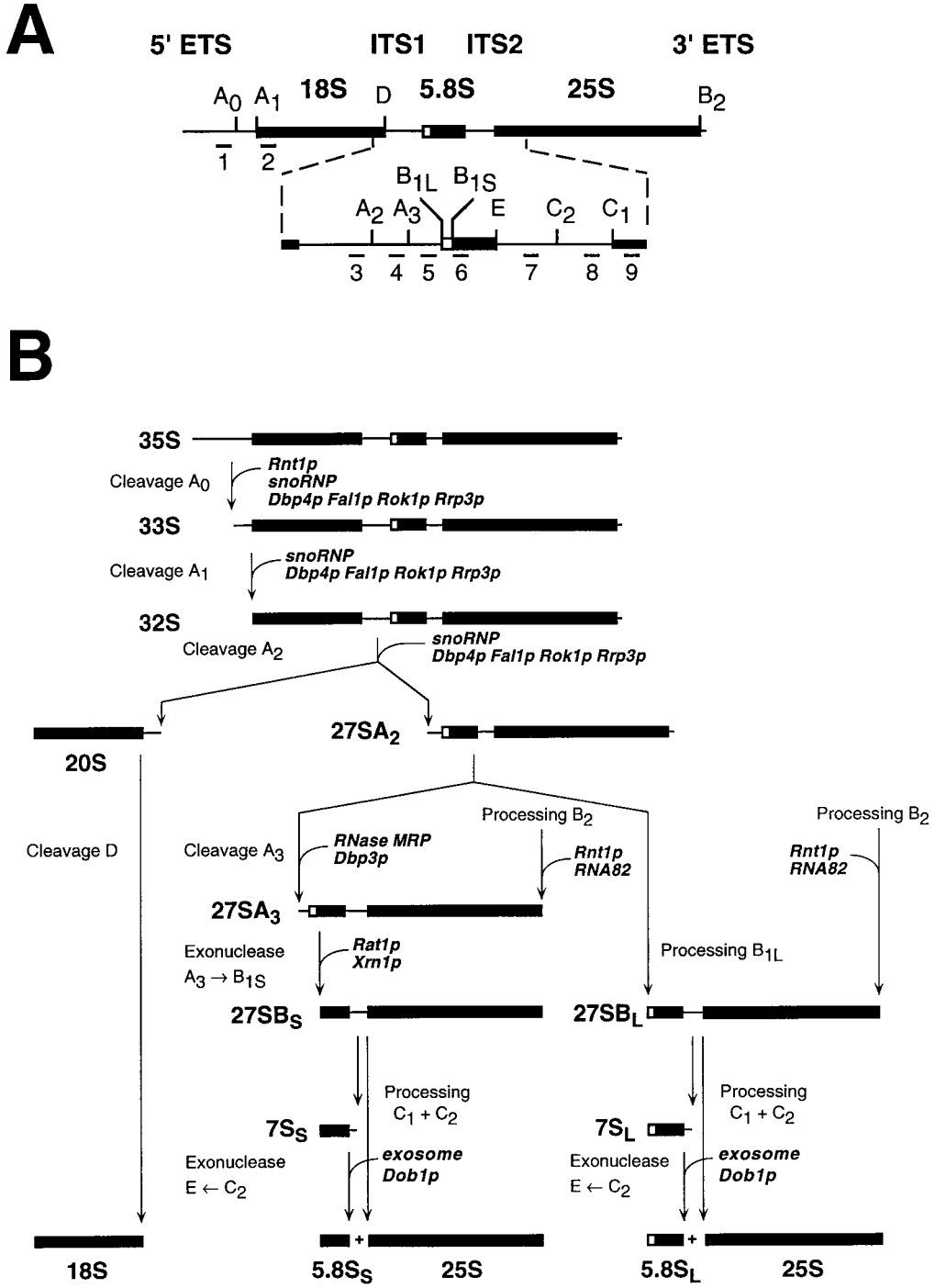

FIG. 1. Scheme of pre-rRNA processing in *S. cerevisiae*. (A) Structure and processing sites of the 35S precursor. This precursor contains the sequences for the mature 18S, 5.8S, and 25S rRNAs, which are separated by two internal transcribed spacers, ITS1 and ITS2. Two external transcribed spacers, 5′ ETS and 3′ ETS, are present at either end. The locations of the various probes (numbered from 1 to 9) used in this study are also indicated. Thick lines represent mature rRNA species, and thin lines represent transcribed spacers. (B) Pre-rRNA processing pathway. The 35S pre-rRNA is cleaved at site A_0 by endonuclease Rnt1p (1), generating the 33S pre-rRNA. This molecule is subsequently processed at sites A_1 and A_2 to give rise to the 20S and $27SA_2$ precursors, resulting in the separation of the pre-rRNAs destined for the small and large ribosomal subunits. It is thought that the early pre-rRNA cleavages from A_0 to A_2 are carried out by a large small nucleolar RNP complex (67), which is likely to be assisted by the putative ATP-dependent RNA helicases Dbp4p (31), Fal1p (28), Rok1p (65), and Rrp3p (41). The final maturation of the 20S precursor takes place in the cytoplasm, where endonucleolytic cleavage at site D yields the mature 18S rRNA. The $27SA_2$ precursor is processed by two alternative pathways that both lead to the formation of mature 5.8S and 25S rRNAs. In the major pathway, the $27SA_2$ precursor is cleaved at site A_3 by RNase MRP (67). The putative ATP-dependent RNA helicase Dbp3p (72) assists in this processing step. The resulting $27SA_3$ precursor is 5′-to-3′ exonucleolytically digested up to site B_{1S} to yield the $27SB_S$ precursor, a reaction requiring exonucleases Xrn1p and Rat1p (21). The minor pathway processes the $27SA_2$ molecule at site B_{1L}, producing the $27SB_L$ pre-rRNA. While processing at site B_1 is completed, the 3′ end of mature 25S rRNA is generated by processing at site B_2. The subsequent ITS2 processing of both 27SB species appears to be identical. Cleavage at sites C_1 and C_2 releases the mature 25S rRNA and the 7S pre-rRNA. The latter undergoes exosome-dependent 3′-to-5′ exonuclease digestion to the 3′ end of the mature 5.8S rRNA (36, 37); this reaction also requires the putative ATP-dependent RNA helicase Dob1p (12). The data presented in this study suggest that Dbp6p is required for the assembly of 60S ribosomal subunits, a process that may also involve three other putative ATP-dependent RNA helicases: Dbp7p (10), Drs1p (44), and Spb4p (49). See references 59 and 67 for reviews on pre-rRNA processing and *trans*-acting factors.

They might be required to provide an accessible sequence in pre-rRNA substrates for proper endonucleolytic processing to take place, as has been suggested for Dbp3p or Fal1p (28, 72), or they could disrupt secondary structures that might otherwise stall or block the activity of an exonuclease, as has been suggested for Dob1p (12). In addition, many snoRNAs, including U3, U14, and the methylation and pseudouridylation guide snoRNAs, form extensive base pair interactions with pre-rRNAs (60). Thus, RNA helicases may play roles in the association or dissociation reactions of these snoRNAs with the pre-rRNA, as has been suggested for Dbp4p and Rok1p (31, 65). Finally, extensive structural rearrangements between pre-rRNAs and r-proteins probably occur during the assembly reactions, and these may require RNA helicases. It is suggested that Dbp7p, Drs1p, and Spb4p are involved in such processes (10, 44, 49).

In this report, we describe the functional analysis of the previously uncharacterized putative ATP-dependent RNA helicase Dbp6p (DEAD-box protein 6). We show that Dbp6p is essential for cell viability and that it localizes to the nucleolus. In vivo depletion of Dbp6p results in a deficit in 60S ribosomal subunits and the appearance of half-mer polysomes. This deficit is accompanied by decreased production of the 27S and 7S precursors, which leads to a decrease in the levels of the mature 25S and 5.8S rRNAs. These phenotypes lead us to conclude that Dbp6p depletion results in improper assembly of preribosomal particles during the biogenesis of 60S ribosomal subunits.

MATERIALS AND METHODS

Strains, media, and genetic methods. The *S. cerevisiae* strains used in this study are derivatives of diploid strain W303 (*MAT***a**/*MAT*α *ura3-1*/*ura3-1 ade2-1*/*ade2-1 his3-11,15*/*his3-11,15 leu2-3,112*/*leu2-3,112 trp1-1*/*trp1-1*) (58). YDK8 (*MAT***a**/*MAT*α *DBP6*/*dbp6::*kanMX4) was obtained by disrupting one *DBP6* open reading frame (ORF) copy with the kanMX4 marker module. YDK8-1A (*MAT*α *dbp6::*kanMX4) is a meiotic segregant of YDK8 that requires a plasmid-borne copy of *DBP6* for cell viability. Preparation of standard media and genetic manipulations were done according to established procedures (4, 26). Yeast cells were transformed by the lithium acetate method (18). One-step gene replacements were done according to Rothstein (45). For tetrad dissection, a Singer MSM micromanipulator was used.

DBP6* disruption.** The deletion disruption of *DBP6* was obtained by transformation of a PCR-synthesized marker cassette with long flanking homology regions into W303 (70, 71). Briefly, the template for LFH1-PCR was genomic DNA prepared from FY1679 (*MATa**/*MAT*α *ura3-52*/*ura3-52 his3*Δ*200*/*HIS3 leu2*Δ*1*/*LEU2 trp1*Δ*63*/*TRP1*) (73). Separate PCRs were set up to obtain the 5′ long flanking homology region (including the start codon and the pFA6a polylinker sequence at its 3′ end) and the 3′ long flanking homology region (including the *DBP6* ORF sequence, starting at +1741, and the pFA6a polylinker sequence at its 5′ end). These LFH1-PCR products were then used as primers to amplify the kanMX4 heterologous marker module from the *Eco*RV-linearized plasmid pFA6a-kanMX4 (71). The LFH2-PCR product was used to directly transform yeast. Selection for transformants was done on yeast extract-peptone-dextrose (YPD) plates containing 200 mg of G418 (Gibco BRL) per liter. Integration at the correct genomic locus was verified by Southern blotting.

The oligonucleotides used with LFH-PCR were P5′ (5′ATT TCA GTC CCA CGA ACT GA3′) (starting 418 bp upstream of the *DBP6* start codon), P5′ long (5′GGG GAT CCG TCG ACC TGC AGC G**CA TTG TCA CTA CCG GTC ACC AAT**3′) (the reverse complement of the *DBP6* start codon is in bold type and underlined, and the *DBP6* 5′ upstream region is in bold type), P3′ long (5′AAA CGA GCT CGA ATT CAT CGA TGA TA**T TCG ATG ACT TAA ACA AAG ATC TA**3′) (the *DBP6* ORF homology region is in bold type and starts 150 bp upstream of the stop codon), and P3′ (5′CAA ACG AGC ATT CCA ACG T3′) (starting 180 bp downstream of the *DBP6* stop codon). For all PCRs, a mixture of *Taq* DNA polymerase (Gibco BRL) and Vent polymerase (New England Biolabs) was used.

Cloning of *DBP6*. The cognate *DBP6* ORF was subcloned from a cosmid (14.22; obtained from P. Philippsen, University of Basel) containing genomic DNA from chromosome XIV. To this end, a 2.79-kb *Sna*BI/*Sac*I fragment was first cloned into the *Eco*RV/*Sac*I-restricted vector pUCBM21 (Boehringer Mannheim Biochemicals) to yield pUCBM21-*DBP6*. Then, a 0.5-kb *Hin*dIII/*Nhe*I fragment and a 2.3-kb *Nhe*I/*Sac*I fragment were excised from pUCBM21-*DBP6* and cloned into the *Hin*dIII/*Sac*I-prepared vector pRS416 (55), resulting in the plasmid pRS416-*DBP6*. Subcloning of a 2.8-kb *Sal*I/*Sac*I fragment into pRS415 (55), YCplac111 (19), and YEplac181 (19) generated the plasmids pRS415-*DBP6*, YCplac111-*DBP6*, and YEplac181-*DBP6*, respectively. The four plasmid constructs complemented the *dbp6* null allele to the wild-type extent.

***DBP6* HA epitope tagging and cloning under the control of a galactose-inducible promoter or a cognate promoter.** *DBP6* was PCR amplified (Vent polymerase) with oligonucleotides introducing the restriction sites *Sal*I (5′GCA CGC GTC GAC **TTT GCA TCG AGA TTT GAC C**3′) (the *Sal*I site is underlined, and the *DBP6* ORF homology region, starting with the second codon, is in bold type) and *Sph*I (5′GCA CAT GCA TGC **CGA GCA TTC CAA CGT GTG**3′) (the *Sph*I site is underlined, and the *DBP6* 3′ downstream homology region, starting 176 bp after the stop codon, is in bold type). The *Sal*I/*Sph*I-restricted PCR product was cloned into the *Sal*I/*Sph*I-cut YCplac111-based plasmid pAS24 (52). The resulting plasmid, pAS24-*DBP6*, contains a *GAL1-GAL10* promoter, a start codon followed by a double hemagglutinin (HA) tag, and the *DBP6* ORF and its 3′-contiguous region. This construct was transformed into strain YDK8-1A (pRS416-*DBP6*), and segregation of the plasmid harboring *URA3 DBP6* (5-fluoroorotic acid selection) resulted in strain YDK8-1A(pAS24-*DBP6*). We also refer to this strain as the *GAL::DBP6* strain or, if grown in YPD medium, as the Dbp6p-depleted strain.

In order to express an N-terminally HA-tagged Dbp6p fusion protein from its cognate promoter at approximately wild-type levels, a fusion PCR was performed (23). Briefly, two fragments with sequence overlap were generated in a first PCR series with *Sac*I-restricted pRS416-*DBP6* as a template and the oligonucleotides 5′AGG GAT AGC CCG CAT AGT CAG GAA CAT CGT ATG GGT ATG **CCA TTG TCA CTA CCG GTC AC**3′ (the *DBP6* ORF homology region and 5′ upstream region are in bold type, and the overlapping part of the double HA tag is underlined), 5′GTA AAA CGA CGG CCA GT3′ (universal primer), 5′TGA CTA TGC GGG CTA TCC CTA TGA CGT CCC GGA CTA TGC A**GG ATC CTT TGC ATC GAG ATT TGA CC**3′ (the *DBP6* ORF homology region is in bold type, the introduced *Bam*HI site is in bold type and underlined, and the overlapping part of the double HA tag is underlined), and P5′int (5′CCT TTC TTG CAA TGA TAC3′) (reverse complement sequence within the *DBP6* ORF, starting at +318) as primers. The PCR products, together with the universal primer and the P5′int primer, were used for the fusion PCR. The final product was cloned as an *Xho*I/*Nhe*I fragment into the *Xho*I/*Nhe*I-restricted plasmid pRS415-*DBP6* to yield plasmid pRS415-*HA-DBP6*. The HA fusion and *DBP6* ORF sequences originating from the fusion PCR were verified by sequencing. This construct complemented the *dbp6* null allele to the wild-type extent, and HA-tagged Dbp6p was detected by Western blotting as a band that migrated at the expected molecular mass of approximately 73 kDa.

Polysome analysis and total ribosomal subunit quantification. Polyribosome preparation, polysome analysis, and ribosomal subunit preparation were done according to Foiani et al. (15) as previously described (28). Gradient analysis was performed with an ISCO UV-6 gradient collector with continuous monitoring at A_{254}.

Indirect immunofluorescence. Strains YDK8-1A(pRS415-*HA-DBP6*) and YDK8-1A(pRS415-*DBP6*) were grown to an optical density at 600 nm (OD_{600}) of about 0.5 in YPD medium, and 5 ml of cells was harvested by centrifugation. Preparation of yeast cells for immunofluorescence was done according to standard procedures (43). DAPI (4′,6-diamidino-2-phenylindole dihydrochloride; Fluka) was used to stain DNA. Primary monoclonal mouse anti-HA antibody 16B12 (BAbCO), at a dilution of 1/1,000, and secondary goat anti-mouse rhodamine-conjugated antibodies (Pierce), at a dilution of 1/200, were used to detect HA-Dbp6p. Polyclonal rabbit anti-Nop1p antibodies (obtained from E. C. Hurt, University of Heidelberg), at a dilution of 1/500, and secondary goat anti-rabbit fluorescein-conjugated antibodies (Pierce), at a dilution of 1/200, were used to detect nucleolar protein Nop1p (61). Fluorescence-labeled cells were inspected in a Zeiss Axiophot fluorescence microscope with the Plan-NEOFLUAR 100×/1.3 objective. Photographs were taken with Kodak TMAX p3200 and transferred to Kodak PhotoCD. Figures were arranged with Adobe Photoshop and printed on a Kodak Digital Science 8650 PS color printer.

Pulse-chase labeling of pre-rRNA. Cells of strains YDK8-1A(pAS24-*DBP6*) and YDK8-1A(pRS415-*DBP6*) were grown in yeast extract peptone galactose (YPGal) medium, shifted to YPD medium, grown in 40 ml of synthetic dextrose (SD) medium lacking methionine (SD-Met) to an OD_{600} of about 1, and concentrated in 1 ml of SD-Met. Cells were then pulse-labeled for 1 min with 250 μCi of [*methyl*-^{3}H]methionine (Amersham; 70 to 85 Ci/mmol). Chase conditions, RNA extraction, and analysis on 1.2% agarose–formaldehyde gels were as previously described (28).

For [5,6-^{3}H]uracil pulse-chase labeling analysis, cells of strains YDK8-1A (pAS24-*DBP6*)(pRS416) and YDK8-1A(pRS416-*DBP6*) were grown in synthetic galactose (SGal)-Ura and then in 40 ml of SD-Ura to an OD_{600} of about 1. The cells were concentrated in 1 ml of SD-Ura and pulse-labeled for 2 min with 100 μCi of [5,6-^{3}H]uracil (Amersham; 45 to 50 Ci/mmol). The chase was initiated by diluting 200-μl aliquots of the pulse-labeled cells in 4 ml of SD medium containing 1 mg of cold uracil per ml. Cells were harvested after 0, 5, 15, 30, and 60 min of chase, washed in ice-cold water, and frozen in liquid nitrogen. Total RNA was extracted by the acid-phenol method (4). Uracil incorporation was measured by scintillation counting, and 30,000 cpm per RNA extract was loaded and resolved on 1.2% agarose–formaldehyde and 7% polyacrylamide–8 M urea gels. RNA was transferred to Hybond-N$^+$ nylon membranes (Amersham) as described previously (28, 66), and the filters were baked for 2 h at 80°C, sprayed

with En^{3}Hance (Du Pont), dried, and exposed to X-ray films for 4 days at −80°C with an intensifying screen.

Northern and primer extension analyses. Steady-state levels of pre-rRNA and mature rRNA were assessed by Northern and primer extension analyses. Oligonucleotides (numbered from 1 to 9 according to the scheme in Fig. 1A) 5′A_0, 18S, D/A_2, A_2/A_3, A_3/B_1, 5.8S, E/C_2, C_1/C_2, and 25S (28) and the oligonucleotide 5S (5′GGT CAC CCA CTA CAC TAC TCG G3′) were end labeled with 30 μCi of [γ-^{32}P]ATP (Amersham; 5,000 Ci/mmol) by use of T4 polynucleotide kinase (Appligene). Total RNA was extracted as described above, and 5 μg was loaded and resolved on 1.2% agarose–formaldehyde gels. For analysis of low-molecular-weight rRNA species, RNA samples (ca. 2.5 μg) corresponding to equal amounts of OD_{600} units of cells were separated on 7% polyacrylamide–8 M urea gels. RNA was transferred to and immobilized on nylon membranes as described above. Prehybridization and hybridization were done with Church buffer (9). Washes were done with 2× SSC (1× SSC is 0.15 M NaCl plus 0.015 M sodium citrate), 0.5% sodium dodecyl sulfate, and 0.1× SSC–0.5% sodium dodecyl sulfate, and the membranes were exposed to X-ray films at −80°C with an intensifying screen.

Primer extension was done with the same RNA samples as those used for Northern analysis according to Venema and Tollervey (68). Oligonucleotides 6 and 7 were used as primers. To identify the positions of the primer extension stops, plasmid-borne rRNA genes were sequenced with the oligonucleotides listed above. Avian myeloblastosis virus reverse transcriptase and RNAguard were purchased from Pharmacia.

Miscellaneous. Total yeast protein extracts were prepared and analyzed by Western blotting according to standard procedures (4, 50). Monoclonal antibody 16B12 and goat anti-mouse alkaline phosphatase-conjugated antibody (Bio-Rad) were used as primary and secondary antibodies, respectively. DNA manipulations were done according to Sambrook et al. (50) with *Escherichia coli* DH10B for subcloning and amplification of plasmid DNA. For dideoxy sequencing, a T7 sequencing kit (Pharmacia) was used. Sequence comparisons were performed at the *Saccharomyces* Genome Database (Stanford University) and NCBI facilities.

RESULTS

Dbp6p is a putative ATP-dependent RNA helicase that is essential for cell viability. *DBP6* (YNR038W) is an ORF of 1,887 bp located on the right arm of *S. cerevisiae* chromosome XIV. The *DBP6* ORF encodes a protein of 629 amino acids with a predicted molecular mass of 70.4 kDa. Dbp6p is also predicted to be acidic (pI, 5.88) and to localize within the cytoplasm (SwissProt Psort program [3]). Calculation of the codon adaptation index (54) suggests that Dbp6p, with a codon adaptation index of 0.19, is of moderate to low intracellular abundance.

Sequence analysis revealed that Dbp6p belongs to the DEAD-box protein family of putative ATP-dependent RNA helicases (Fig. 2). Seven of the eight conserved motifs characteristic of DEAD-box proteins are present in Dbp6p. Like all other DEAD-box proteins from yeast, with the exception of Tif1/2p (33) and Fal1p (28), Dbp6p also has relatively large N- and C-terminal extensions to the helicase core region. The N-terminal domain contains an 86-amino-acid region (amino acids 39 to 124) that is highly enriched in aspartic acid (11.6% versus 5.4% for the full-length protein), glutamic acid (23.2% versus 6.5%), and serine (20.9% versus 10.8%) residues, but it does not contain many positively charged amino acids (Fig. 2).

As a first approach to the functional analysis of Dbp6p, we constructed a *dbp6* null allele. We replaced most of one *DBP6* ORF copy in the diploid strain W303 with the kanMX4 marker module (see Materials and Methods). Correct integration at the genomic locus was verified by Southern blotting. Subsequent tetrad analysis showed a 2:2 segregation of viable to nonviable spores, with all the viable progeny being *DBP6* and G418 sensitive (data not shown). The Δ*dbp6* spores germinated, but cell division stopped after three to five generations. The cognate *DBP6* ORF complemented its null allele after transformation of the *DBP6*/*dbp6*::kanMX4 heterozygote (YDK8) with pRS416-*DBP6* and subsequent sporulation and tetrad analyses (data not shown). Furthermore, Dbp6p was required for vegetative growth, as judged by the lack of growth of YDK8-1A(pRS416-*DBP6*) on 5-fluoroorotic acid-containing plates (data not shown). These results showed that Dbp6p is essential for cell viability.

```
1
M F A S R F D P S Q L T A P A A S A P E G I V G T T P P A I
V P L K R Q A T E S D N E E Y G S H Q D S D E S S N S S S E
E D E D R M Q V D Y G A S E E D S S E V E E E E S K P S T H
S T V L S R F K Q T V S L Q E R L G A S D I A E S K E D E G
I E D E A A S T H Q L K Q I P Q P E F V K N P M N L N T N S
L Q F K S T G W L N T E K I Y Y D N S L I K P F S D Y A N E
L E A K L L Q N I C K N F S T N T F P I Q S I I L D S I L P
V L N F T L N V S K R N F T R R I G D I L V N A A T G S G K
T L A Y S I P I V Q T L F K R Q I N R L R C I I I V P T K L
L I N Q V Y T T L T K L T Q G T S L I V S I A K L E N S L K
D E H K K L S N L E P D I L I T T P G R L V D H L N M K S I
N L K N L K F L I I D E A D R L L N Q S F Q G W C P K L M S
H L K T D K L D T L P G N V I K M I F S A T L T T N T E K L
N G L N L Y K P K L F L K Q T D K L Y Q L P N K L N E F N I
N I P T A K S V Y K P L I L L Y S I C Q F M A H S P I A A K
I L I F V K S N E S S I R L S K L L Q L I C E S R S Q S S V
L K N L Q N L A V S I N S V N S N N S K A E N K K I V A N F
S H H S E S A G I T I L I T T D I M S R G I D I N D I T Q V
I N Y D P P M S S Q Q Y V H R V G R T A R A N E L G S A Y N
L L V G R G E R T F F D D L N K D L D R D G K S V Q P L E L
D F T L L E S D S E L Y T S S L E S L K N Y H N N T A Q A *
                                                    629
```

FIG. 2. *DBP6* encodes a putative ATP-dependent RNA helicase of the DEAD-box protein family. Seven of the eight conserved motifs characteristic of DEAD-box proteins are found in Dbp6p (bold type and underlined). The helicase core region extends from amino acid 234 (A motif) to amino acid 598 (HRVGR motif). A portion of the N-terminal domain, starting at amino acid 39 and ending at amino acid 124, is highly enriched in serine and the negatively charged amino acids aspartic acid and glutamic acid (underlined).

Construction of a *GAL::DBP6* strain. To determine the essential Dbp6p function, a conditional system for phenotypic analysis was established. The *DBP6* ORF and its 3′ downstream sequence were cloned under the control of a galactose-inducible promoter, which allows gene expression in medium containing galactose (YPGal) and represses gene expression in glucose-based medium (YPD). The resulting plasmid, pAS24-*DBP6*, expressed an N-terminally HA-tagged Dbp6p that complemented the *dbp6* null mutant (YDK8-1A) on YPGal plates to the wild-type extent and resulted in a strong slow-growth phenotype on YPD plates at 30°C (data not shown). After YDK8-1A(pAS24-*DBP6*) was shifted from YPGal medium to YPD medium, the growth rate remained similar to that of the wild-type control strain YDK8-1A(YCplac111-*DBP6*) for the first 12 h but then progressively decreased to a doubling time of more than 8 h after 36 h in YPD medium (Fig. 3A). Concomitant with the decrease in the growth rate, the cells were depleted of HA-Dbp6p, as detected by Western blot analysis (Fig. 3B).

In vivo depletion of Dbp6p leads to a deficiency in 60S ribosomal subunits. As some DEAD-box proteins are involved in either translation initiation (6, 8, 11) or ribosome biogenesis (28, 44, 72), we first investigated by polysome profile analysis whether Dbp6p was involved in one of these two processes. For this purpose, YDK8-1A(pAS24-*DBP6*) was grown at 30°C in YPGal medium and shifted to YPD medium, and then polysomes were extracted at different times. Wild-type polysome profiles were obtained after 6 h (Fig. 4A). Concomitant with the decrease in the growth rate and in HA-Dbp6p levels after 24 h, the Dbp6p-depleted strain showed a deficit of free 60S versus 40S ribosomal subunits, an overall decrease in 80S ribosomes (free couples and monosomes) and polysomes, and an accumulation of half-mer polysomes (Fig. 4B). The 60S-

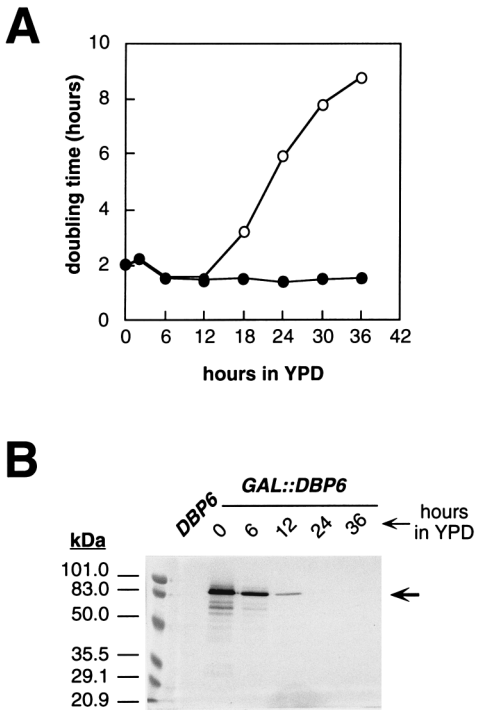

FIG. 3. Growth of yeast cells is impaired upon Dbp6p depletion. (A) Growth curves for YDK8-1A(pAS24-*DBP6*) (*GAL::DBP6*; open circles) and YDK8-1A(YCplac111-*DBP6*) (*DBP6*; closed circles) at 30°C after logarithmic cultures were shifted from YPGal medium to YPD medium for up to 36 h. Data are given as doubling times at different times in YPD medium. (B) Depletion of Dbp6p. Cell extracts of the *GAL::DBP6* strain were prepared from samples harvested at the indicated times. The cell extract of the *DBP6* strain was prepared from a sample harvested after 36 h in YPD medium. Extracts were assayed by Western blot analysis with monoclonal mouse anti-HA antibody 16B12. Equal amounts of protein (ca. 70 μg) were loaded in each lane, as judged by Coomassie blue staining of gels or red Ponceau staining of blots (data not shown). Prestained markers (Bio-Rad) were used as standards for molecular mass determinations. The HA-Dbp6p signal is indicated by an arrow. No signal was detected for untagged Dbp6p.

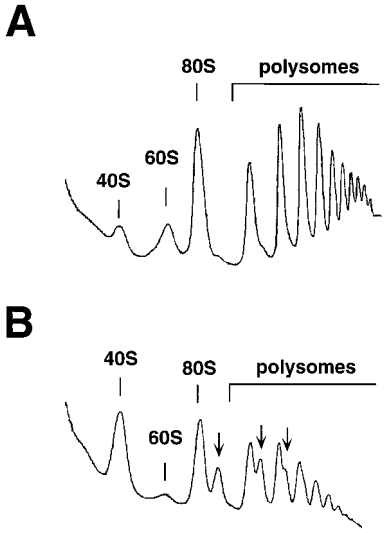

FIG. 4. Depletion of Dbp6p results in a deficiency in 60S ribosomal subunits. YDK8-1A(pAS24-*DBP6*) was grown in YPGal medium and shifted to YPD medium for up to 24 h. Polysome analysis was done after 6 h (A) and 24 h (B). Cell extracts were resolved in 7 to 50% sucrose gradients. The peaks of free 40S and 60S ribosomal subunits, 80S ribosomes (free couples and monosomes), and polysomes are indicated. Half-mer polysomes are indicated by arrows.

ribosomal-subunit deficit was confirmed by quantifying total ribosomal subunits in polysome runoff and low-Mg^{2+} cell extracts. The 60S-to-40S ratio was determined from the A_{254}. It was about 1.9 for the wild-type control strain YDK8-1A (YCplac111-*DBP6*); this ratio was about 1.5 for YDK8-1A (pAS24-*DBP6*) after 24 h of Dbp6p depletion. Thus, polysome analysis indicated that Dbp6p plays a role in the metabolism of 60S ribosomal subunits.

Dbp6p localizes to the nucleolus. To distinguish between a cytoplasmic role and a nucleolar role of Dbp6p, the subcellular localization of Dbp6p was analyzed by indirect immunofluorescence. For this purpose, *DBP6* was HA tagged at its 5′ end by fusion PCR and cloned into pRS415 to express the N-terminally epitope-tagged Dbp6p from its cognate promoter at approximately wild-type levels (see Materials and Methods). The resulting plasmid (pRS415-*HA-DBP6*) or a control plasmid harboring the untagged *DBP6* gene (pRS415-*DBP6*) was transformed into strain YDK8-1A(pRS416-*DBP6*). Upon plasmid shuffling and subsequent restreaking on YPD plates, HA-Dbp6p complemented the *dbp6* null allele to the wild-type extent at all temperatures tested (16, 30, and 37°C). In addition, Western blot analysis with an anti-HA antibody detected a single protein with the expected molecular mass of ca. 73 kDa in a total cell extract from a strain expressing HA-tagged Dbp6p [YDK8-1A(pRS415-*HA-DBP6*)] but not from a strain expressing untagged Dbp6p [YDK8-1A(pRS415-*DBP6*)] (data not shown). The two strains were grown in YPD medium to an OD_{600} of about 0.5, and cells were processed for immunofluorescence. The HA-tagged Dbp6p was detected by anti-HA antibodies, followed by decoration with goat anti-mouse rhodamine-conjugated antibodies (Fig. 5A). For precise localization, the nucleus was visualized by staining of DNA with DAPI (Fig. 5C) and the nucleolus was stained with anti-Nop1p antibodies in combination with goat anti-rabbit fluorescein-conjugated antibodies (Fig. 5B). The fluorescence photographs demonstrated that HA-Dbp6p is restricted to the nucleolus (Fig. 5A), where it colocalizes with Nop1p (Fig. 5B). In most cells, Dbp6p and Nop1p showed the typical crescentic or cap-like staining pattern of nucleolar proteins. No signal was obtained with the combination of anti-HA and goat anti-mouse rhodamine-conjugated antibodies when cells of strain YDK8-1A(pRS415-*DBP6*) were analyzed by indirect immunofluorescence (data not shown). The predominant localization of HA-Dbp6p in the nucleolus, the specialized compartment for ribosome biosynthesis (35), indicated that Dbp6p is implicated in the biogenesis of 60S ribosomal subunits.

Formation of the mature 25S and 5.8S rRNAs is impaired upon Dbp6p depletion. To study the role of Dbp6p in 60S-

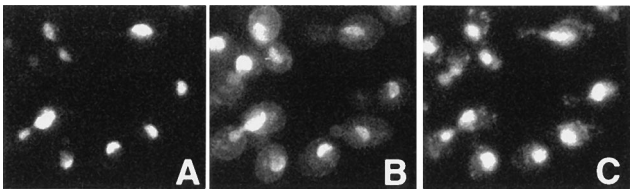

FIG. 5. HA-Dbp6p localizes to the nucleolus. Indirect immunofluorescence was performed with cells expressing HA-Dbp6p from the *DBP6* promoter [YDK8-1A(pRS415-*HA-DBP6*)]. (A) HA-Dbp6p was detected with monoclonal mouse anti-HA antibody 16B12, followed by decoration with goat anti-mouse rhodamine-conjugated antibodies. (B) Nop1p was detected with polyclonal rabbit anti-Nop1p antibodies, followed by decoration with goat anti-rabbit fluorescein-conjugated antibodies. (C) Chromatin DNA was stained with DAPI.

ribosomal-subunit biogenesis, we first analyzed the effects of Dbp6p depletion on the synthesis and processing of pre-rRNA by [*methyl*-^{3}H]methionine pulse-chase labeling experiments. For this purpose, YDK8-1A(pAS24-*DBP6*) and the wild-type control strain YDK8-1A(pRS415-*DBP6*) were grown first as logarithmic cultures in YPGal medium, then for 12 h in YPD medium, and finally for another 10 h to an OD_{600} of about 1 in SD-Met. At this time, the *GAL::DBP6* strain was doubling every 5.5 h, compared to 2.5 h for the wild-type strain. The cells were pulse-labeled for 1 min and then chased for 2, 5, and 15 min with an excess of cold methionine. We observed a net decrease in the ratio of labeled 25S to 18S mature rRNAs in the Dbp6p-depleted strain relative to the wild-type strain (Fig. 6A, lanes 3, 4, 7, and 8). Furthermore, processing of the 35S precursor was slightly delayed, and practically no 32S precursor was formed. Interestingly, different bands of high molecular weight appeared at the 1-min pulse time point. These bands presumably correspond to 35S pre-rRNA-derived intermediates or degradation products that became metastable in the absence of Dbp6p. Moreover, less of the 27S species formed, with the 27SA and 27SB precursors not persisting until the 2-min chase time point (Fig. 6A, lanes 5 and 6). The formation of the 18S rRNA was also weakly impaired, as revealed by the lower levels of its 20S precursor and the mature species itself and by the accumulation of an aberrant 23S species (Fig. 6A, lanes 5 and 6). However, the kinetics of processing of the 20S precursor to the mature 18S rRNA seemed not to be affected.

To exclude a defect in rRNA methylation and to monitor the processing and formation of low-molecular-weight RNAs, cells were also pulse-labeled with [5,6-^{3}H]uracil. Strains YDK8-1A (pAS24-*DBP6*)(pRS416) and YDK8-1A(pRS416-*DBP6*) were grown first as logarithmic cultures in SGal-Ura and then for 22 h in SD-Ura to an OD_{600} of about 1. At this time, the *GAL::DBP6* strain was doubling every 4.5 h, compared to 2.75 h for the wild-type strain. The cells were pulse-labeled for 2 min and then chased for 5, 15, 30, and 60 min with an excess of cold uracil. Results comparable to those shown in Fig. 6A were obtained after total RNA samples were analyzed by agarose gel electrophoresis (data not shown), thus excluding an rRNA methylation defect following Dbp6p depletion. Analysis of low-molecular-weight RNAs by polyacrylamide gel electrophoresis showed that the synthesis of mature 5.8S rRNA was substantially reduced upon Dbp6p depletion. The synthesis of 5S rRNA and the labeling of tRNAs, however, were comparable in both kinetics and levels in wild-type and Dbp6p-depleted cells (Fig. 6B). Altogether, these results indicated that the deficit in 60S ribosomal subunits following Dbp6p depletion was due to impaired precursor formation or stability, which led to reduced synthesis of both mature 25S and mature 5.8S rRNAs.

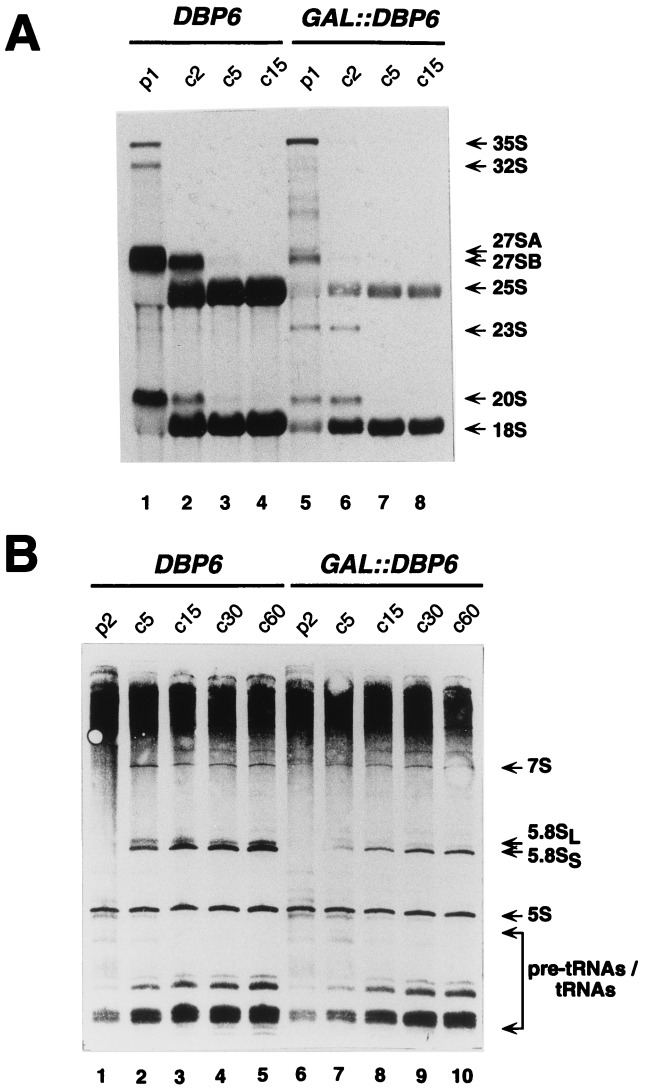

FIG. 6. Dbp6p depletion leads to reduced synthesis of the mature 25S and 5.8S rRNAs. (A) Wild-type control strain YDK8-1A(YCplac111-*DBP6*) (*DBP6*) and strain YDK8-1A(pAS24-*DBP6*) (*GAL::DBP6*) were grown at 30°C in YPGal medium, shifted for 12 h to YPD medium, and then grown for 10 h in SD-Met. Cells were pulse-labeled (p) for 1 min with [*methyl*-^{3}H]methionine and then chased (c) for 2, 5, and 15 min with an excess of unlabeled methionine. Total RNA was extracted, and 20,000 cpm was loaded and separated on a 1.2% agarose–formaldehyde gel, transferred to a nylon membrane, and visualized by fluorography. (B) Strains YDK8-1A(pRS416-*DBP6*) (*DBP6*) and YDK8-1A (pAS24-*DBP6*)(pRS416) (*GAL::DBP6*) were grown at 30°C in SGal-Ura and then shifted to SD-Ura for 22 h. Cells were pulse-labeled (p) for 2 min with [5,6-^{3}H]uracil and then chased (c) for 5, 15, 30, and 60 min with an excess of unlabeled uracil. Total RNA was extracted, and 30,000 cpm was loaded and separated on a 7% polyacrylamide–8 M urea gel, transferred to a nylon membrane, and visualized by fluorography. The positions of the different pre-rRNAs, mature rRNAs, and tRNAs are indicated.

Dbp6p is required for normal pre-rRNA processing. To define the pre-rRNA processing steps that are affected upon Dbp6p depletion, steady-state levels of pre-rRNA and mature rRNA were determined by Northern blot and primer extension analyses. Different oligonucleotides hybridizing to defined regions of the 35S pre-rRNA transcript (Fig. 1A) were used to monitor specific processing intermediates in a wild-type control strain and during a time course of Dbp6p depletion. Depletion of Dbp6p resulted in a slight decrease in 18S rRNA and a more drastic decrease in 25S rRNA steady-state levels (Fig. 7A). Probing with oligonucleotide 1 (Fig. 7B), which hybridizes 5′ to site A_0, revealed that the *GAL::DBP6* strain accumulated, with ongoing depletion of Dbp6p, an aberrant processing product that had already been detected by the pulse-chase labeling experiments. This aberrant species could also be detected with oligonucleotides 3 (Fig. 7C) and 4 (Fig. 7D) but not with oligonucleotide 5 (Fig. 7E), indicating that this rRNA molecule might extend from the 5′ end of the 5′ ETS to the A_3 site and thus correspond to the previously described aberrant 23S processing product (67). Concomitant with Dbp6p depletion, the amounts of the 32S pre-rRNA (Fig. 7D) and the 20S pre-rRNA (Fig. 7C) diminished slightly. More importantly, the $27SA_2$ and 27SB pre-rRNAs were strongly depleted (Fig. 7D to F; data not shown for oligonucleotide 8).

To assess the steady-state levels of low-molecular-weight

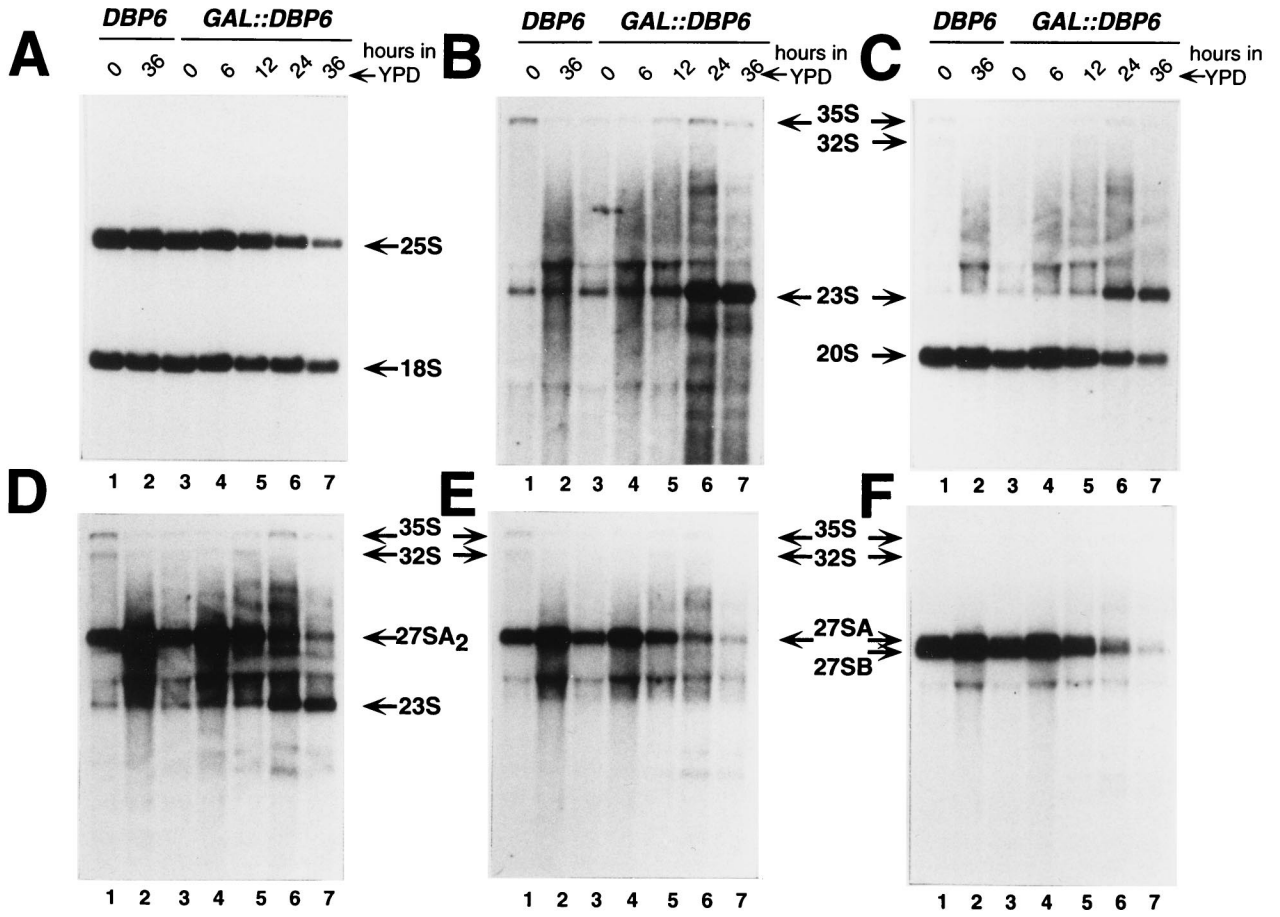

FIG. 7. Dbp6p depletion leads to lower steady-state levels of the 27S precursors and the mature 25S rRNA. Strains YDK8-1A(pRS416-*DBP6*) (*DBP6*) and YDK8-1A(pAS24-*DBP6*) (*GAL::DBP6*) were grown in YPGal medium and shifted to YPD medium for up to 36 h. The cells were harvested at the indicated times. Total RNA was extracted, separated on a 1.2% agarose–formaldehyde gel, transferred to a nylon membrane, and subjected to Northern analysis. The same filter was consecutively hybridized with the probes indicated in Fig. 1A. (A) Oligonucleotides 2 and 9, base pairing to sequences within the mature 18S and 25S rRNAs, respectively. (B) Oligonucleotide 1 in 5′ ETS. (C) Oligonucleotide 3 in ITS1 between sites D and A_2. (D) Oligonucleotide 4 in ITS1 between sites A_2 and A_3. (E) Oligonucleotide 5 in ITS1 downstream of site A_3. (F) Oligonucleotide 7 in ITS2 between sites E and C_2. The positions of the different pre-rRNAs and mature rRNAs are indicated.

rRNAs, samples were separated on polyacrylamide gels and subjected to Northern blot analysis with 7S-, 5.8S-, and 5S-specific oligonucleotides. Hybridizations indicated that the 7S pre-rRNA was strongly depleted (Fig. 8, top panel) and that the levels of the mature 5.8S rRNA were also decreased (Fig. 8, middle panel). However, the steady-state levels of the 5S rRNA were only very slightly affected by Dbp6p depletion (Fig. 8, bottom panel).

Because Northern hybridization poorly detects mature $5.8S_L$ rRNA and because it does not distinguish between the $27SA_3$ and $27SA_2$ precursors and between the $27SB_L$ and $27SB_S$ precursors, we assessed the levels of these species by primer extension. This analysis confirmed that Dbp6p depletion led to a net decrease in all the 27S precursors, with the 27SB species being most drastically affected (Fig. 9A), and to diminished levels of both mature $5.8S_L$ and mature $5.8S_S$ rRNAs (Fig. 9B). Furthermore, primer extension showed that processing at all sites tested was correct at the nucleotide level during the time course of Dbp6p depletion.

Altogether, our results demonstrate that Dbp6p depletion leads to decreased formation and decreased steady-state levels of the 27S and 7S precursors and, as a consequence, of the mature 25S and 5.8S rRNAs. These phenotypes may be due to or may cause an improper assembly of preribosomal particles during the biogenesis of 60S ribosomal subunits. The nucleolar localization of HA-Dbp6p and the 60S-ribosomal-subunit deficiency upon Dbp6p depletion are in agreement with a proposed role of Dbp6p in 60S-ribosomal-subunit biogenesis.

DISCUSSION

In this paper, we describe the functional analysis of Dbp6p, a putative ATP-dependent RNA helicase of the DEAD-box protein family. Disruption analysis showed that Dbp6p is essential for cell viability. In vivo depletion of Dbp6p resulted in a deficit in 60S ribosomal subunits, which led to the appearance of half-mer polysomes. Similar polysome profiles have been described for mutants defective in r-proteins of the 60S ribosomal subunit (13, 39, 69) and for mutants defective in components involved in pre-rRNA processing and 60S-ribosomal-subunit assembly (24, 44, 56, 72, 75). Since we detected N-terminally HA-tagged Dbp6p only in the nucleolus, we concluded that Dbp6p is not a structural component of 60S ribosomal subunits but rather plays a role in their biogenesis. Interestingly, Dbp6p is predicted to be cytoplasmic and lacks a consensus nuclear localization signal. This finding may indicate

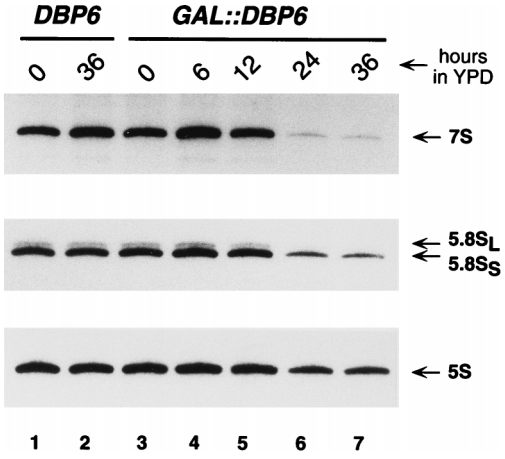

FIG. 8. Dbp6p depletion leads to lower steady-state levels of the 7S precursor and the mature 5.8S rRNAs. Strains YDK8-1A(pRS416-*DBP6*) (*DBP6*) and YDK8-1A(pAS24-*DBP6*) (*GAL::DBP6*) were grown in YPGal medium and shifted to YPD medium for up to 36 h. The cells were harvested at the indicated times. Total RNA was extracted, separated on a 7% polyacrylamide–8 M urea gel, transferred to a nylon membrane, and subjected to Northern analysis. The same filter was consecutively hybridized with three different probes: oligonucleotide 7 in ITS2 between sites E and C_2 (top panel); oligonucleotide 6, base pairing to sequences within the mature 5.8S rRNAs (middle panel); and oligonucleotide 5S, base pairing to sequences within the mature 5S rRNA (bottom panel). The positions of the 7S pre-rRNA and the mature 5.8S and 5S rRNAs are indicated.

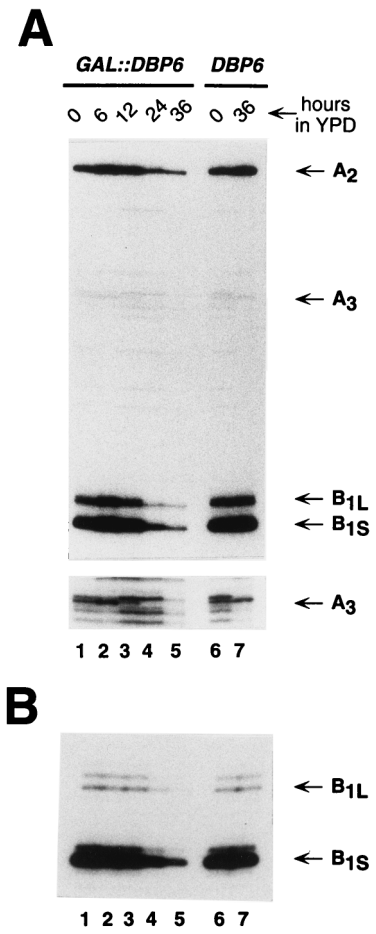

FIG. 9. Primer extension analysis of the 27S precursors and the mature 5.8S rRNAs. Strains YDK8-1A(pRS416-*DBP6*) (*DBP6*) and YDK8-1A(pAS24-*DBP6*) (*GAL::DBP6*) were grown in YPGal medium and shifted to YPD medium for up to 36 h. The cells were harvested at the indicated times, and total RNA was extracted. (A) Primer extension with oligonucleotide 7 in ITS2 reveals processing sites B_{1S}, B_{1L}, A_3, and A_2. The bottom panel is a longer exposure of the same gel, and it shows the A_3 site. (B) Primer extension with oligonucleotide 6, priming within the mature 5.8S rRNAs. The positions of the primer extension stops corresponding to the different pre-rRNA species and the mature 5.8S rRNAs are indicated.

that Dbp6p carries an as-yet-unknown signal sequence for nuclear targeting or that it is imported into the nucleus by binding to a nucleus-targeted protein in the cytoplasm.

To define the role of Dbp6p in the biogenesis of 60S ribosomal subunits, we investigated the formation and steady-state levels of pre-rRNA and mature rRNA by pulse-chase labeling, Northern blotting, and primer extension analyses. Pulse-chase labeling of pre-rRNA showed that the synthesis of the mature 25S and 5.8S rRNAs was quantitatively diminished and kinetically delayed compared to the formation of the mature 18S and 5S rRNAs. Processing of the 35S precursor was slightly delayed, and practically no 32S precursor was detected. Most notably, different high-molecular-weight species, most likely corresponding to 35S pre-rRNA-derived degradation products, could be detected during the pulse. We propose that the processed 35S pre-rRNA might not have been stable in the absence of Dbp6p and, as a consequence, that less of the 27S species was formed. Furthermore, the stability of the 27S precursors was probably also affected because they did not persist until the first chase time point. Moreover, the formation of the 18S rRNA was also weakly impaired, as revealed by the appearance of the aberrant 23S processing product and by the lower levels of the 20S precursor and of the mature 18S rRNA species.

The results of the pulse-chase labeling experiments were confirmed by Northern blotting and primer extension analyses, which showed that the steady-state levels of the 27SA and, more drastically, of the 27SB precursors were decreased. As a consequence, the 7S pre-rRNA was strongly depleted, and reduced steady-state levels of the mature 25S and 5.8S rRNAs were detected. In agreement with the finding that newly synthesized 5S rRNA is more stable than 5.8S rRNA upon depletion of the 60S-subunit protein L16 (38), the steady-state levels of the 5S rRNA were only very slightly affected by Dbp6p depletion. We conclude that Dbp6p is required for the normal formation of 25S and 5.8S rRNAs. The amounts of both the 32S and the 20S pre-rRNAs also were diminished slightly, and the aberrant 23S species, which is the product of direct cleavage of the 35S pre-rRNA at site A_3 when processing at sites A_0, A_1, and A_2 is delayed or inhibited, accumulated. These findings could implicate Dbp6p in 18S rRNA synthesis; however, this role would only be a minor one, since the steady-state levels of both the 40S ribosomal subunit and the 18S rRNA were less affected than the steady-state levels of the 60S ribosomal subunit and the mature 25S or 5.8S rRNA. In agreement with these findings, reduced processing of the 35S precursor, accumulation of the aberrant 23S species, and some depletion of the 20S pre-rRNA and the 18S rRNA have been reported for different mutants affecting 60S-ribosomal-subunit biogenesis (5, 12, 24, 72, 75). Thus, delayed processing at sites A_0, A_1, and A_2 may be a general feature of mutations that interfere with the synthesis of mature 25S and 5.8S rRNAs. The mechanism is unclear; however, it is likely that all of the processing machinery interacts to some extent or that there is some form of feedback inhibition due to defective 25S and 5.8S rRNA synthesis. Indeed, the biogenesis of mature 40S ribosomal units

and the biogenesis of mature 60S ribosomal subunits are not independent events. Instead, processing of the 35S pre-rRNA requires the assembly of this primary transcript into a ribonucleoprotein particle, 90S RNP, which contains many r-proteins of the mature 40S and 60S ribosomal subunits as well as nonribosomal proteins that are most likely *trans*-acting factors involved in pre-rRNA processing or ribosome assembly reactions (63). Furthermore, functional interactions between the processing machinery responsible for cleavages at sites A_0, A_1, and A_2 (small nucleolar RNP complex) and that responsible for cleavage at site A_3 (RNase MRP complex) have been reported, and they probably occur via the bridging factor Rrp5p (2, 68).

In addition to Dbp6p, other proteins have been shown to be required for 60S-ribosomal-subunit biogenesis. All of these proteins can be arbitrarily grouped into two classes. The first class consists of *trans*-acting factors that are directly involved in pre-rRNA processing reactions and includes the endonucleolytic RNase MRP complex, the exonucleases Xrn1p and Rat1p, the exosome, and the putative ATP-dependent RNA helicases Dbp3p and Dob1p (see Fig. 1B and its legend for further information and references). In contrast, the precise functional roles of proteins belonging to the second class are not clear. This class includes nucleolar and r-proteins that are required for proper ribosome assembly. Mutations in or in vivo depletion of Nip7p, Nop2p, Nop3p, and the r-proteins L1 and L32 lead to an accumulation of one of the 27S precursors (13, 24, 47, 69, 75), while in vivo depletion of Nop4p/Nop77p results in some depletion of 27SA and, more drastically, of 27SB pre-rRNAs (5, 56). The phenotype observed after the depletion of Dbp6p most closely resembles that described for Nop4/Nop77p-depleted strains (5, 56). In both cases, early cleavage at sites A_0 to A_2 is kinetically delayed, but the most striking effect is the large decrease in 27SB pre-rRNA levels. In contrast, the depletion of Nop4p/Nop77p but not of Dbp6p impairs rRNA methylation. We conclude that Dbp6p, like Nop4p/Nop77p, plays a primary role in the early ribosome assembly steps leading to the formation of mature 60S ribosomal subunits. Considering its presumed RNA helicase activity, Dbp6p could function in the unwinding of the pre-rRNA to promote specific intramolecular rRNA or rRNA-protein interactions. An abortive assembly of the pre-RNP in the absence of Dbp6p would then either be the cause or the consequence of the instability and rapid turnover of the 27S pre-rRNAs. The increased stability of these 27S precursors observed during the depletion of Nip7p, Nop2p, and Nop3p strongly suggests that these *trans*-acting factors are involved in ribosome assembly steps downstream of the ones assisted by Nop4p/Nop77p and Dbp6p. This involvement may occur at a point where the assembly of 60S ribosomal subunits is close to completion and assembly would more likely be arrested rather than aborted (24).

In agreement with a 60S-ribosomal-subunit assembly function for Dbp6p, we obtained predominantly cold-sensitive *dbp6* mutants (at 18°C) by random PCR mutagenesis. When examined by polysome profile analysis, all of these mutants displayed a 60S-ribosomal-subunit deficiency phenotype similar to that observed upon Dbp6p depletion (29). It has been argued on the basis of thermodynamic grounds that mutations affecting assembly reactions may be intensified at low temperatures (7). Indeed, many cold-sensitive alleles blocking ribosome assembly have been found in bacteria (20, 57). Furthermore, cold-sensitive DEAD-box protein mutations that affect bacterial and yeast ribosome assembly have been identified (40, 44, 49, 62, 72).

The functional analysis of Dbp6p reported here is, to our knowledge, the first report that clearly implicates a putative ATP-dependent RNA helicase in the assembly of 60S ribosomal subunits in *S. cerevisiae*. However, earlier publications suggested, based on polysome profile analyses and pulse-chase labeling experiments, that mutations in two other putative ATP-dependent RNA helicases, Drs1p and Spb4p, also affect 60S-ribosomal-subunit assembly (44, 49). Unfortunately, the destiny of the 27S pre-rRNAs in *drs1* and *spb4* mutants has not been assessed so far. As Dbp6p, Drs1p, and Spb4p are all essential for cell viability, it is unlikely that they carry out redundant functions. More recently, it was also shown that Dbp7p, a nonessential putative ATP-dependent RNA helicase, may also assist in early 60S-ribosomal-subunit assembly reactions (10). However, experimental evidence indicates that Dbp6p and Dbp7p are not genetically redundant (10, 29). We conclude that there are at least four putative ATP-dependent RNA helicases that play nonredundant roles in the assembly of 60S ribosomal subunits. It will be interesting to determine what their precise functions are and why so many putative RNA helicases are needed in this process. Thus, it will be crucial to determine whether these proteins exhibit RNA unwinding or RNA-dependent ATPase activities and what their specific RNA substrates are.

ACKNOWLEDGMENTS

We thank M. Rekik for technical assistance, E. C. Hurt for the kind gift of the anti-Nop1p antibodies, and M.-C. Daugeron for communicating results prior to publication. We are grateful to D. Tollervey, J. Venema, and members of our laboratory for fruitful discussions, and we are grateful to M.-C. Daugeron, I. Iost, and K. Tanner for critical reading of the manuscript. We are indebted to M. Collart and U. Oberholzer for providing us with plasmid pRS416-*DBP6*. Special thanks are due to B. Emery for his contribution and enthusiasm during a 2-month practical stay in our laboratory.

We are grateful to C. Georgopoulos for supporting our work. J.C. acknowledges a fellowship from the Spanish government (Ministerio de Educación y Ciencia) and support from Sandoz-Stiftung and Ciba-Geigy Jubiläums-Stiftung. The initial parts of this study also were supported by the Swiss Federal Office for Education and Science. This work was supported by grant 31-43321.95 from the Swiss National Science Foundation to P.L.

REFERENCES

1. **Abou Elela, S., H. Igel, and M. Ares, Jr.** 1996. RNase III cleaves eukaryotic preribosomal RNA at a U3 snoRNP-dependent site. Cell **85:**115–124.
2. **Allmang, C., Y. Henry, J. P. Morrissey, H. Wood, E. Petfalski, and D. Tollervey.** 1996. Processing of the yeast pre-rRNA at sites A_2 and A_3 is linked. RNA **2:**63–73.
3. **Appel, R. D., A. Bairoch, and D. F. Hochstrasser.** 1994. A new generation of information retrieval tools for biologists: the example of the ExPASy WWW server. Trends Biochem. Sci. **19:**258–260.
4. **Ausubel, F. M., R. Brent, R. E. Kingston, D. D. Moore, J. G. Seidman, J. A. Smith, and K. Struhl.** 1994. Current protocols in molecular biology, vol. 2, p. 13.0.1–13.14.17. John Wiley & Sons, Inc., New York, N.Y.
5. **Bergès, T., E. Petfalski, D. Tollervey, and E. C. Hurt.** 1994. Synthetic lethality with fibrillarin identifies NOP77p, a nucleolar protein required for pre-rRNA processing and modification. EMBO J. **13:**3136–3148.
6. **Blum, S., M. Mueller, S. R. Schmid, P. Linder, and H. Trachsel.** 1989. Translation in *Saccharomyces cerevisiae*: initiation factor 4A-dependent cell-free system. Proc. Natl. Acad. Sci. USA **86:**6043–6046.
7. **Cantor, C. R., and P. R. Schimmel.** 1980. Biophysical chemistry, part I, p. 287–288. W. H. Freeman & Co., San Francisco, Calif.
8. **Chuang, R.-Y., P. L. Weaver, Z. Liu, and T.-H. Chang.** 1997. Requirement of the DEAD-box protein Ded1p for messenger RNA translation. Science **275:** 1468–1471.
9. **Church, G. M., and W. Gilbert.** 1984. Genomic sequencing. Proc. Natl. Acad. Sci. USA **81:**1991–1995.
10. **Daugeron, M.-C., and P. Linder.** Dbp7p, a putative ATP-dependent RNA helicase from *Sarcharomyces cerevisiae*, is required for 60S ribosomal subunit assembly. Submitted for publication.
11. **de la Cruz, J., I. Iost, D. Kressler, and P. Linder.** 1997. The p20 and Ded1 proteins have antagonistic roles in eIF4E-dependent translation in *Saccharomyces cerevisiae*. Proc. Natl. Acad. Sci. USA **94:**5201–5206.

12. **de la Cruz, J., D. Kressler, D. Tollervey, and P. Linder.** Dob1p (Mtr4p) is a putative ATP-dependent RNA helicase required for the 3′ end formation of 5.8S rRNA in *Saccharomyces cerevisiae*. EMBO J., in press.
13. **Deshmukh, M., Y.-F. Tsay, A. G. Paulovich, and J. L. Woolford, Jr.** 1993. Yeast ribosomal protein L1 is required for the stability of newly synthesized 5S rRNA and the assembly of 60S ribosomal subunits. Mol. Cell. Biol. **13:** 2835–2845.
14. **Eichler, D. C., and N. Craig.** 1994. Processing of eukaryotic ribosomal RNA. Prog. Nucleic Acid Res. Mol. Biol. **49:**197–239.
15. **Foiani, M., A. M. Cigan, C. J. Paddon, S. Harashima, and A. G. Hinnebusch.** 1991. GCD2, a translational repressor of the *GCN4* gene, has a general function in the initiation of protein synthesis in *Saccharomyces cerevisiae*. Mol. Cell. Biol. **11:**3203–3216.
16. **Fuller-Pace, F. V.** 1994. RNA helicases: modulators of RNA structure. Trends Cell Biol. **4:**271–274.
17. **Fuller-Pace, F. V., S. M. Nicol, A. D. Reid, and D. P. Lane.** 1993. DbpA: a DEAD box protein specifically activated by 23S rRNA. EMBO J. **12:**3619–3626.
18. **Gietz, D., A. St. Jean, R. A. Woods, and R. H. Schiestl.** 1992. Improved method for high efficiency transformation of intact yeast cells. Nucleic Acids Res. **20:**1425.
19. **Gietz, R. D., and A. Sugino.** 1988. New yeast-*Escherichia coli* shuttle vectors constructed with in vitro mutagenized yeast genes lacking six-base pair restriction sites. Gene **74:**527–534.
20. **Guthrie, C., H. Nashimoto, and M. Nomura.** 1969. Structure and function of *E. coli* ribosomes. VIII. Cold-sensitive mutants defective in ribosome assembly. Proc. Natl. Acad. Sci. USA **63:**384–391.
21. **Henry, Y., H. Wood, J. P. Morrissey, E. Petfalski, S. Kearsey, and D. Tollervey.** 1994. The 5′ end of yeast 5.8S rRNA is generated by exonucleases from an upstream cleavage site. EMBO J. **13:**2452–2463.
22. **Hirling, H., M. Scheffner, T. Restle, and H. Stahl.** 1989. RNA helicase activity associated with the human p68 protein. Nature **339:**562–564.
23. **Ho, S. N., H. D. Hunt, R. M. Horton, J. K. Pullen, and L. R. Pease.** 1989. Site-directed mutagenesis by overlap extension using the polymerase chain reaction. Gene **77:**51–59.
24. **Hong, B., J. S. Brockenbrough, P. Wu, and J. P. Aris.** 1997. Nop2p is required for pre-rRNA processing and 60S ribosome subunit synthesis in yeast. Mol. Cell. Biol. **17:**378–388.
25. **Jacobs Anderson, J. S., and R. Parker.** 1996. RNA turnover: the helicase story unwinds. Curr. Biol. **6:**780–782.
26. **Kaiser, C., S. Michaelis, and A. Mitchell.** 1994. Methods in yeast genetics: a laboratory course manual. Cold Spring Harbor Laboratory Press, Cold Spring Harbor, N.Y.
27. **Kim, S.-H., J. Smith, A. Claude, and R.-J. Lin.** 1992. The purified yeast pre-mRNA splicing factor PRP2 is an RNA-dependent NTPase. EMBO J. **11:**2319–2326.
28. **Kressler, D., J. de la Cruz, M. Rojo, and P. Linder.** 1997. Fal1p is an essential DEAD-box protein involved in 40S-ribosomal-subunit biogenesis in *Saccharomyces cerevisiae*. Mol. Cell. Biol. **17:**7283–7294.
29. **Kressler, D., B. Emery, and P. Linder.** 1997. Unpublished data.
30. **Liang, L., W. Diehl-Jones, and P. Lasko.** 1994. Localization of vasa protein to the *Drosophila* pole plasm is independent of its RNA-binding and helicase activities. Development **120:**1201–1211.
31. **Liang, W.-Q., J. A. Clark, and M. J. Fournier.** 1997. The rRNA-processing function of the yeast U14 small nucleolar RNA can be rescued by a conserved RNA helicase-like protein. Mol. Cell. Biol. **17:**4124–4132.
32. **Linder, P., P. F. Lasko, M. Ashburner, P. Leroy, P. J. Nielsen, K. Nishi, J. Schnier, and P. P. Slonimski.** 1989. Birth of the D-E-A-D box. Nature **337:** 121–122.
33. **Linder, P., and P. P. Slonimski.** 1989. An essential yeast protein, encoded by duplicated genes *TIF1* and *TIF2* and homologous to the mammalian translation initiation factor eIF-4A, can suppress a mitochondrial missense mutation. Proc. Natl. Acad. Sci. USA **86:**2286–2290.
34. **Margossian, S. P., and R. A. Butow.** 1996. RNA turnover and the control of mitochondrial gene expression. Trends Biochem. Sci. **21:**392–396.
35. **Mélèse, T., and Z. Xue.** 1995. The nucleolus: an organelle formed by the act of building a ribosome. Curr. Opin. Cell Biol. **7:**319–324.
36. **Mitchell, P., E. Petfalski, A. Shevchenko, M. Mann, and D. Tollervey.** 1997. The exosome: a conserved eukaryotic RNA processing complex containing multiple 3′→5′ exoribonucleases. Cell **91:**457–466.
37. **Mitchell, P., E. Petfalski, and D. Tollervey.** 1996. The 3′ end of yeast 5.8S rRNA is generated by an exonuclease processing mechanism. Genes Dev. **10:** 502–513.
38. **Moritz, M., A. G. Paulovich, Y.-F. Tsay, and J. L. Woolford, Jr.** 1990. Depletion of yeast ribosomal proteins L16 or rp59 disrupts ribosome assembly. J. Cell Biol. **111:**2261–2274.
39. **Moritz, M., B. A. Pulaski, and J. L. Woolford, Jr.** 1991. Assembly of 60S ribosomal subunits is perturbed in temperature-sensitive yeast mutants defective in ribosomal protein L16. Mol. Cell. Biol. **11:**5681–5692.
40. **Nishi, K., F. Morel-Deville, J. W. B. Hershey, T. Leighton, and J. Schnier.** 1988. An eIF-4A-like protein is a suppressor of an *Escherichia coli* mutant defective in 50S ribosomal subunit assembly. Nature **336:**496–498.
41. **O'Day, C. L., F. Chavanikamannil, and J. Abelson.** 1996. 18S rRNA processing requires the RNA helicase-like protein Rrp3. Nucleic Acids Res. **24:** 3201–3207.
42. **Pause, A., and N. Sonenberg.** 1993. Helicases and RNA unwinding in translation. Curr. Opin. Struct. Biol. **3:**953–959.
43. **Pringle, J. R., A. E. M. Adams, D. G. Drubin, and B. K. Haarer.** 1991. Immunofluorescence methods for yeast, p. 565–602. *In* C. Guthrie and G. R. Fink (ed.), Guide to yeast genetics and molecular biology. Academic Press, Inc., San Diego, Calif.
44. **Ripmaster, T. L., G. P. Vaughn, and J. L. Woolford, Jr.** 1992. A putative ATP-dependent RNA helicase involved in *Saccharomyces cerevisiae* ribosome assembly. Proc. Natl. Acad. Sci. USA **89:**11131–11135.
45. **Rothstein, R. J.** 1983. One-step gene disruption in yeast. Methods Enzymol. **101:**202–211.
46. **Rozen, F., I. Edery, K. Meerovitch, T. E. Dever, W. C. Merrick, and N. Sonenberg.** 1990. Bidirectional RNA helicase activity of eucaryotic translation initiation factors 4A and 4F. Mol. Cell. Biol. **10:**1134–1144.
47. **Russell, I. D., and D. Tollervey.** 1992. NOP3 is an essential yeast protein which is required for pre-rRNA processing. J. Cell Biol. **119:**737–747.
48. **Rymond, B. C., and M. Rosbash.** 1992. Yeast pre-mRNA splicing, p. 143–192. *In* E. W. Jones, J. R. Pringle, and J. R. Broach (ed.), The molecular and cellular biology of the yeast *Saccharomyces*, vol. 2. Gene expression. Cold Spring Harbor Laboratory Press, Cold Spring Harbor, N.Y.
49. **Sachs, A. B., and R. W. Davis.** 1990. Translation initiation and ribosomal biogenesis: involvement of a putative rRNA helicase and RPL46. Science **247:**1077–1079.
50. **Sambrook, J., E. F. Fritsch, and T. Maniatis.** 1989. Molecular cloning: a laboratory manual, 2nd ed. Cold Spring Harbor Laboratory Press, Cold Spring Harbor, N.Y.
51. **Schmid, S. R., and P. Linder.** 1992. D-E-A-D protein family of putative RNA helicases. Mol. Microbiol. **6:**283–292.
52. **Schmidt, A., M. Bickle, T. Beck, and M. N. Hall.** 1997. The yeast phosphatidylinositol kinase homolog TOR2 activates RHO1 and RHO2 via the exchange factor ROM2. Cell **88:**531–542.
53. **Schwer, B., and C. Guthrie.** 1991. PRP16 is an RNA-dependent ATPase that interacts transiently with the spliceosome. Nature **349:**494–499.
54. **Sharp, P. M., E. Cowe, D. G. Higgins, D. C. Shields, K. H. Wolfe, and F. Wright.** 1988. Codon usage patterns in *Escherichia coli*, *Bacillus subtilis*, *Saccharomyces cerevisiae*, *Schizosaccharomyces pombe*, *Drosophila melanogaster* and *Homo sapiens*; a review of the considerable within-species diversity. Nucleic Acids Res. **16:**8207–8211.
55. **Sikorski, R. S., and P. Hieter.** 1989. A system of shuttle vectors and yeast host strains designed for efficient manipulation of DNA in *Saccharomyces cerevisiae*. Genetics **122:**19–27.
56. **Sun, C., and J. L. Woolford, Jr.** 1994. The yeast *NOP4* gene product is an essential nucleolar protein required for pre-rRNA processing and accumulation of 60S ribosomal subunits. EMBO J. **13:**3127–3135.
57. **Tai, P.-C., D. P. Kessler, and J. Ingraham.** 1969. Cold-sensitive mutations in *Salmonella typhimurium* which affect ribosome synthesis. J. Bacteriol. **97:** 1298–1304.
58. **Thomas, B. J., and R. Rothstein.** 1989. Elevated recombination rates in transcriptionally active DNA. Cell **56:**619–630.
59. **Tollervey, D.** 1996. *Trans*-acting factors in ribosome synthesis. Exp. Cell Res. **229:**226–232.
60. **Tollervey, D., and T. Kiss.** 1997. Function and synthesis of small nucleolar RNAs. Curr. Opin. Cell Biol. **9:**337–342.
61. **Tollervey, D., H. Lehtonen, M. Carmo-Fonseca, and E. C. Hurt.** 1991. The small nucleolar RNP protein NOP1 (fibrillarin) is required for pre-rRNA processing in yeast. EMBO J. **10:**573–583.
62. **Toone, W. M., K. E. Rudd, and J. D. Friesen.** 1991. *deaD*, a new *Escherichia coli* gene encoding a presumed ATP-dependent RNA helicase, can suppress a mutation in *rpsB*, the gene encoding ribosomal protein S2. J. Bacteriol. **173:** 3291–3302.
63. **Trapman, J., J. Retèl, and R. J. Planta.** 1975. Ribosomal precursor particles from yeast. Exp. Cell Res. **90:**95–104.
64. **van Nues, R. W., J. Venema, J. M. J. Rientjes, A. Dirks-Mulder, and H. A. Raué.** 1995. Processing of eukaryotic pre-rRNA: the role of the transcribed spacers. Biochem. Cell Biol. **73:**789–801.
65. **Venema, J., C. Bousquet-Antonelli, J.-P. Gelugne, M. Caizergues-Ferrer, and D. Tollervey.** 1997. Rok1p is a putative RNA helicase required for rRNA processing. Mol. Cell. Biol. **17:**3398–3407.
66. **Venema, J., R. J. Planta, and H. A. Raué.** 1997. *In vivo* mutational analysis of ribosomal RNA in *Saccharomyces cerevisiae. In* R. Martin (ed.), Protein synthesis: methods and protocols, in press. Humana Press, Totowa, N.J.
67. **Venema, J., and D. Tollervey.** 1995. Processing of pre-ribosomal RNA in *Saccharomyces cerevisiae*. Yeast **11:**1629–1650.
68. **Venema, J., and D. Tollervey.** 1996. *RRP5* is required for formation of both 18S and 5.8S rRNA in yeast. EMBO J. **15:**5701–5714.
69. **Vilardell, J., and J. R. Warner.** 1997. Ribosomal protein L32 of *Saccharomyces cerevisiae* influences both the splicing of its own transcript and the processing of rRNA. Mol. Cell. Biol. **17:**1959–1965.
70. **Wach, A.** 1996. PCR-synthesis of marker cassettes with long flanking homol-

ogy regions for gene disruptions in *S. cerevisiae*. Yeast **12:**259–265.
71. **Wach, A., A. Brachat, R. Pöhlmann, and P. Philippsen.** 1994. New heterologous modules for classical or PCR-based gene disruptions in *Saccharomyces cerevisiae*. Yeast **10:**1793–1808.
72. **Weaver, P. L., C. Sun, and T.-H. Chang.** 1997. Dbp3p, a putative RNA helicase in *Saccharomyces cerevisiae*, is required for efficient pre-rRNA processing predominantly at site A_3. Mol. Cell. Biol. **17:**1354–1365.
73. **Winston, F., C. Dollard, and S. L. Ricupero-Hovasse.** 1995. Construction of a set of convenient *Saccharomyces cerevisiae* strains that are isogenic to S288C. Yeast **11:**53–55.
74. **Woolford, J. L., Jr., and J. R. Warner.** 1991. The ribosome and its synthesis, p. 587–626. *In* J. R. Broach, J. R. Pringle, and E. W. Jones (ed.), The molecular and cellular biology of the yeast *Saccharomyces*, vol. 1. Genome dynamics, protein synthesis, and energetics. Cold Spring Harbor Laboratory Press, Cold Spring Harbor, N.Y.
75. **Zanchin, N. I. T., P. Roberts, A. DeSilva, F. Sherman, and D. S. Goldfarb.** 1997. *Saccharomyces cerevisiae* Nip7p is required for efficient 60S ribosome subunit biogenesis. Mol. Cell. Biol. **17:**5001–5015.